Nanostructured Zinc Sulphide Thin Films

M.A. Jafarov, E.F. Nasirov, S.A.Jahangirova, R.Jafarli
Baku State University, Baku, Azerbaijan, maarif.jafarov@mail.ru

Abstract---ZnS thin films are prepared by pulsed laser deposition and the effect of annealing temperature on the structural and optical properties of ZnS films is investigated systematically using techniques like X-ray diffraction (XRD), Atomic force microscopy (AFM), UV-VIS spectroscopy and Photoluminescence spectroscopy (PL).

– – – – – – – – – – ◆ – – – – – – – – – –

1.INTRODUCTION

As an important II-VI semiconductor, with wide band gap energy of 3.7 eV, ZnS has been extensively studied due to its important applications in electronics and photonics [1-4] including light-emitting diodes, flat-panel displays, and photonic crystal devices, which operate in the region from visible to near infrared. Because of high refractive index (2.35) and high transmittance in the visible range, ZnS can be used as a reflector and dielectric filter in the area of optics [5, 6]. ZnS is a potentially important material to be used as an antireflection coating for heterojunction solar cells [7]. It is an important device material for the detection, emission and modulation of visible and near ultraviolet light [8, 9]. In recent years, nanocrystalline ZnS have attracted much attention because the properties in nanoforms differ significantly from those of their bulk counter parts. Therefore, much effort has been made to control size, morphology and polycrystallinity of the ZnS nanocrystals with a view to tune their physical properties [10]. There are several deposition techniques to grow ZnS thin films including sputtering [11,12], metal oraganic chemical vapour deposition [13], molecular beam epitaxy [14], atomic layer epitaxy [15], spray pyrolysis [16] and pulsed laser deposition [17,18]. Among them, PLD has been reported to have numerous advantages over the classical deposition methods because in PLD, one can control size distribution and shape of nanocrystals by varying the parameters like target to substrate distance, laser fluence, background gas pressure, substrate temperature etc. Thus it emerges as an effective tool for the growth of quantum structures with high chemical purity and controlled stoichiometry [19]. In this paper, we report the deposition of ZnS nanostructured films by on-axis pulsed laser ablation and the effect of post deposition annealing on the structural and optical

properties of ZnS thin films are investigated using XRD, AFM, UV-visible spectroscopy and photoluminescence spectroscopy.

2. EXPERIMENTAL DETAILS

ZnS thin films are prepared by pulsed laser deposition technique (PLD). The deposition of the films is carried out inside a multiport stainless steel vacuum chamber equipped with a gas inlet, a rotating multi-target and a heatable substrate holder. The irradiations are performed using a Q-switched Nd: YAG laser (Quanta – Ray INDI – series, Spectra Physics) with 200 mJ of laser energy at frequency doubled 532 nm radiation, having pulse width of 7 ns and repetition frequency of 10 Hz. The ZnS target was prepared from high purity (99.99%) ZnS powder (Sigma Aldrich). Three grams of ZnS powder is weighed accurately and ground well in an agate mortar with a pestle. Two or three drops of polyvinyl alcohol (PVA) are added to ensure proper binding of the material. Thoroughly ground powder is then heated at 373 K for 45 minutes in a muffle furnace to remove water. The pressed pellet is scintered at a temperature of 1300 ^{0}C for 24 hours. This pellet is used as the target for laser deposition of the films. Quartz substrates are used for film preparation. Before irradiations, the deposition chamber is evacuated down to a base pressure of $4x10^{-6}$ mbar using a diffusion pump and two rotary pumps. The depositions of the films are done for duration of 30 minutes on quartz substrates kept at an on-axis distance of 4 cm from the target in vacuum condition. The laser radiation is impinged on the target at 45 ^{0} with respect to normal. The deposited films are annealed at four different temperatures viz., 300, 400, 500 and 600 ^{0}C. The target is rotated with constant speed during ablation to avoid pitting of target at any given spot and to obtain uniform thin films.

The crystalline structure and crystallographic orientations of the films are characterized by X-Ray Diffraction (XPERT PRO Diffractometer). Surface morphology of the deposited films at nanometric scale is investigated by AFM (Digital Instruments Nanoscope III, Si_3N_4 100µ cantilever, 0.58 N/m force constant) measurements in contact mode. Grain size and root mean square (rms) surface roughness of the deposited films are determined on an area of 1 x 1 µm using the instrument associated with the instrument. The optical transmission and reflection spectroscopic measurements are performed for the wavelength range of 200-900 nm using JASCO

V-550 UV-Visible double beam spectrophotometer. Photoluminescence spectra of the samples are recorded by Horiba Jobin Yvon Flourolog III modular spectroflourometer equipped with 450 W Xenon lamp and Hamatsu R928-28 photomultiplier with a computer attached to the setup. The thickness of the films is determined by using Stylus profilometer.

3. RESULTS AND DISCUSSION

Fig.1 shows XRD pattern of the films as a function of annealing temperature. It is observed that the as-deposited and annealed films show polycrystalline nature and have hexagonal wurtzite phase. The XRD peaks of the films annealed at temperatures from 300 ^{0}C to 500 ^{0}C show enhanced intensity compared to that of the as-deposited films indicating the improvement in crystallinity for the annealed films. The as-deposited film shows only random orientation of film growth whereas the film annealed at 300 ^{0}C show a preferred orientation along the (0 0 $\underline{14}$) direction. For the films annealed at 400 and 500 ^{0}C, preferred orientation change to (1 1 $\underline{18}$) and (0 2 8) planes respectively. When the films are annealed at 600 ^{0}C, the intensity of the peaks reduced considerably without showing any preferred orientation. The XRD pattern of the film annealed at 400 ^{0}C show an intense peak for the plane (0 0 20). In the XRD pattern of the film annealed at 500 ^{0}C this peak remains absent and a new intense XRD peak for the reflection plane (1 0 $\underline{11}$) observed. In the XRD pattern for the film annealed at 600 ^{0}C the peak corresponding to the reflection plane (0 0 $\underline{20}$) show weak intensity where as peak for the plane (0 0 $\underline{11}$) remains absent. The XRD patterns (Fig.1) reveal that annealing temperature has profound effect on the structural properties of ZnS films.

Zhang et al., have reported that when the ZnS films are annealed at a temperature 500 ^{0}C or above, the ZnS begins a transformation to ZnO. The XRD pattern of the film annealed at 600 ^{0}C show a less intense XRD peak at 2θ value = 36.249 ^{0} corresponding to the lattice plane (1 0 1) of hexagonal ZnO. This observation indicates that the sulfur sites of wurtzite ZnS are replaced by oxygen during the thermal annealing process. The oxygen atoms diffuse into the ZnS matrix via interstitial sites and bond to zinc, forcing sulphur atoms to occupy the interstitial sites in turn, and leading to a modification of the hexagonal unit network [20].

The average size of the crystalline grains in the films is estimated by the following Debye Scherrer equation

$$D_{hkl} = \frac{0.9\lambda}{\beta_{hkl}\cos(\theta_{hkl})} \qquad (1)$$

where λ is the X-ray wavelength, θ_{hkl} is the Bragg diffraction angle and β_{hkl} is the full width at half- maximum (FWHM) in radian of the main peak in the X-ray diffraction pattern. The calculated grain sizes vary from 11 to 32 nm and are found to be nanocrystalline. From the Table 1, it can be observed that, as the annealing temperature increases the grain size decreases and then increases. Usually on annealing smaller grains coalease into bigger grains. The observed decrease in grain size with increase in annealing temperature is interesting. The decrease in intensity levels

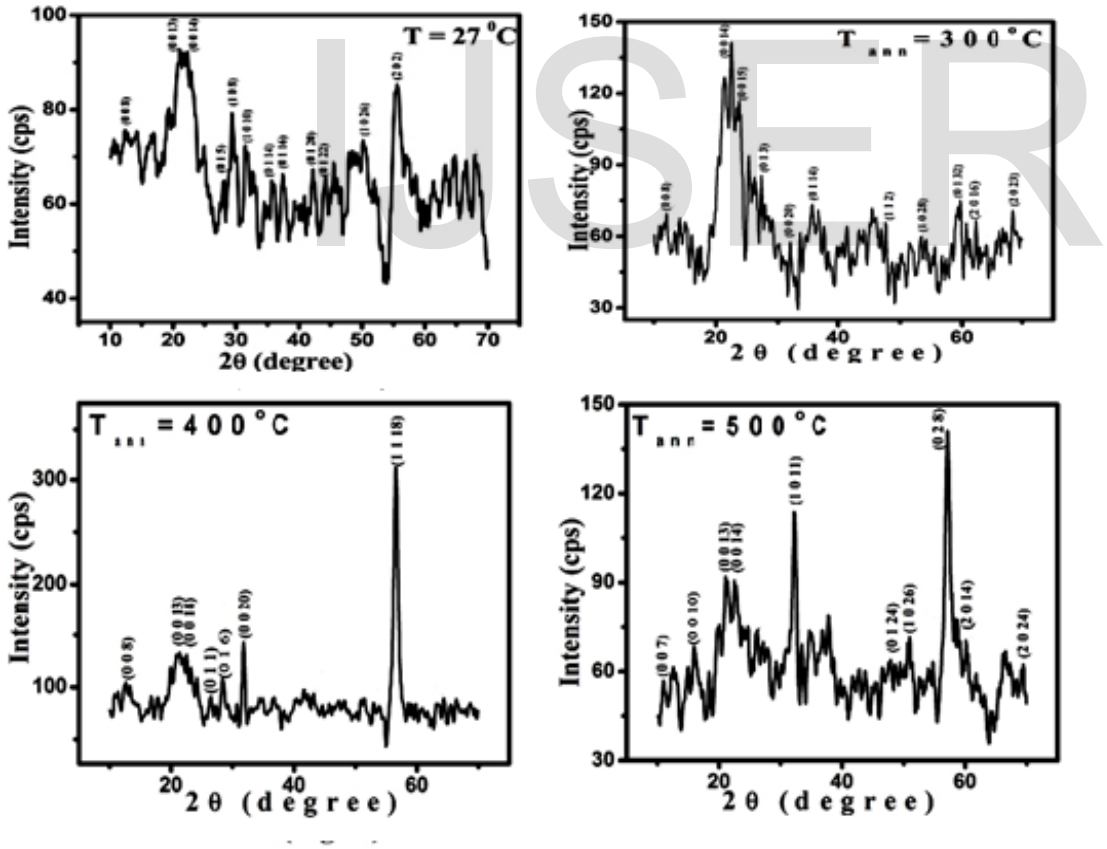

Fig.1 XRD pattern of pulsed laser ablated as-deposited and post annealed ZnS thin films

occurring when films are annealed at higher temperature may be explained interms of formation of mixed phases in these samples. For a hexagonal system, the d-spacing is related to the lattice parameters by the following equation

$$\frac{1}{d^2} = \frac{4}{3}\left(\frac{h^2 + hk + k^2}{a^2}\right) + \frac{l^2}{c^2} \qquad (2)$$

where h, k and l are the miller indices and a, b and c are the lattice parameters along x, y and z directions. For the ZnS bulk sample the lattice constants reported are a = b = 3.8230 and c = 56.200 A^0 (JCPDS Card No. 83-2124). The calculated lattice constants are shown in Table 1 and they match with the standard values. This supports our observation that the films prepared under non reactive atmosphere have hexagonal wurtzite structure of the ZnS.

To study the effect of annealing temperature on the surface properties systematically, AFM measurements have been performed on all films on a scan area of 1 x 1 µm. Fig.2 shows the 3D AFM images of the as-deposited and post-annealed films at different annealing temperatures viz, 300, 400, 500 and 600 ^{0}C respectively.

The AFM pictures show the uniform distribution of grains of identical sizes with well defined grain boundaries in the as-deposited film. The film annealed at 300 ^{0}C shows denser, compact and uniform distribution of particles of lesser size compared to that of the as-deposited film. The film annealed at 400 ^{0}C show the distribution of bigger grains with more porosity and less well defined grain boundary. The AFM pictures of films annealed at 500 ^{0}C show uniform distribution of particles of slightly lesser size compared to that of the film annealed at 400 ^{0}C. Also the film annealed at 500 ^{0}C seems to be less porous compared to that of the film annealed at 400 ^{0}C. AFM pictures of the film annealed at 600 ^{0}C show denser distribution of grains of different sizes. This observation is in support of the XRD observation that the film contains both ZnS and ZnO phases. The rms surface roughness of the as-deposited and annealed ZnS films are estimated and are shown in Table 1. A systematic increase of rms surface roughness with increase in annealing temperature can be observed and it is shown in Fig. 3. The surface of the annealed films becomes rough, which is expected for polycrystalline film formation.

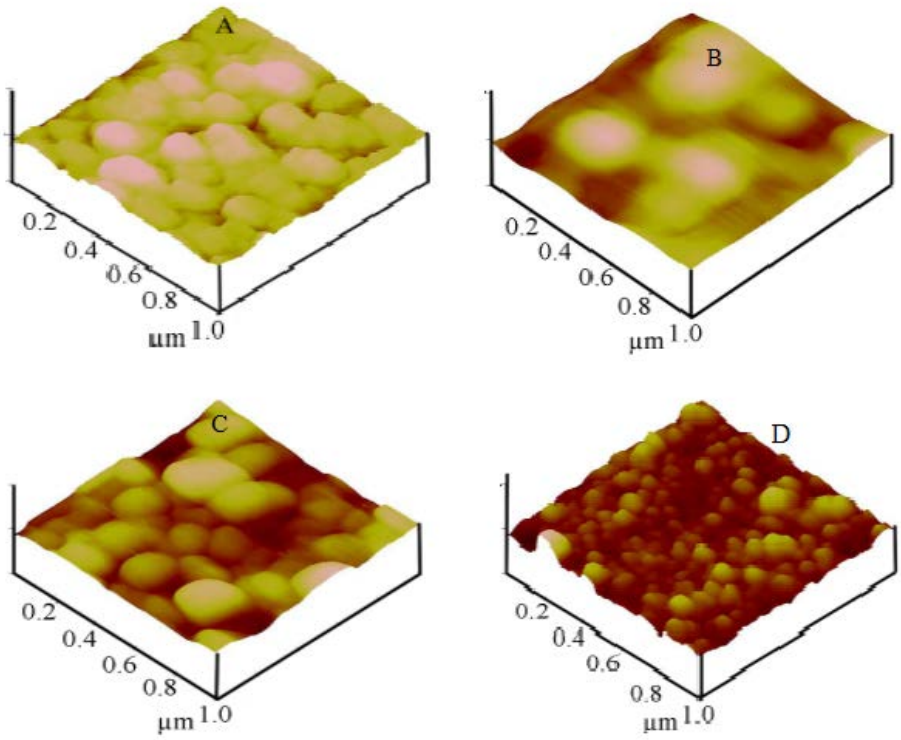

Fig.2 AFM images of laser ablated nanostructured ZnS thin films (A) as-deposited and annealed at temperatures (B) 300 ^{0}C (C) 400 ^{0}C and (D) 500 ^{0}C

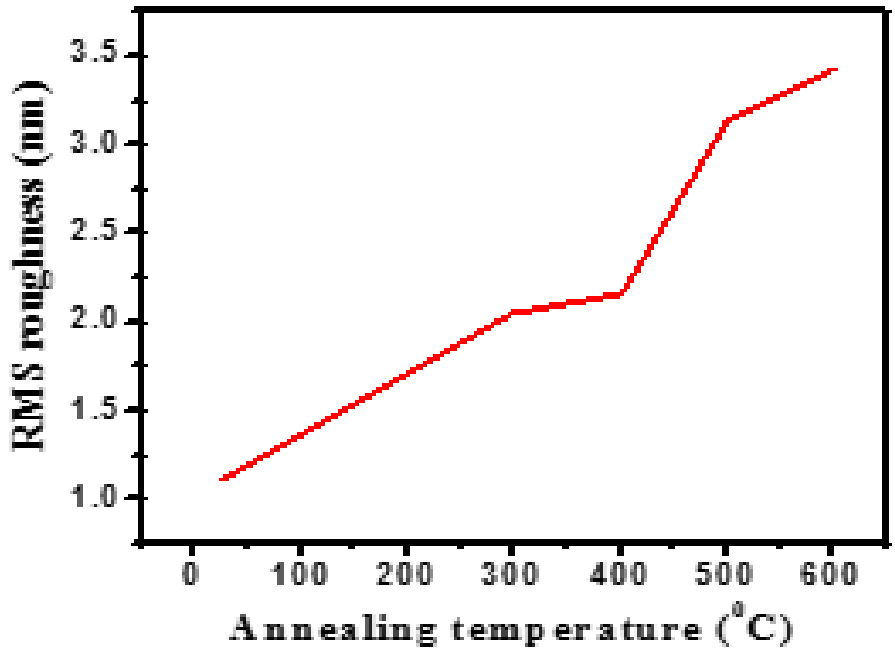

Fig.3 Variation of rms roughness with annealing temperature

Fig.4 shows the optical transmittance spectra of as-deposited and post annealed ZnS thin films prepared under vacuum condition. As deposited ZnS thin films show a transmittance of ~54 %, which is decreased to a value of 30% for films annealed at 300 ^{0}C. The films annealed at 400 and 600 ^{0}C show enhanced transmittance above 60%. The film annealed at 500^{0}C show the highest transmittance of ~ 80%. Below 400 nm there is a sharp fall of transmittance for all the films, which is due to the strong absorption of light by the films in this region and this corresponds to the intrinsic band edge of the films. The reduction in the transmittance of the film, on annealing to 300 ^{0}C is quite intriguing. On annealing the film get more ordered and become more crystalline and one can expect better transparency. The average size of the grains in the as-deposited film and the film annealed at 300 ^{0}C from the XRD measurements are 32 nm and 18 nm respectively. The reduction of particle size should also lead to improved transparency of the film. The AFM pictures show that the film annealed at 300 ^{0}C are denser and less porous, and consist of uniform distribution of smaller particles compared to that of the as-deposited film. These properties also should have improved the transparency of the annealed films.

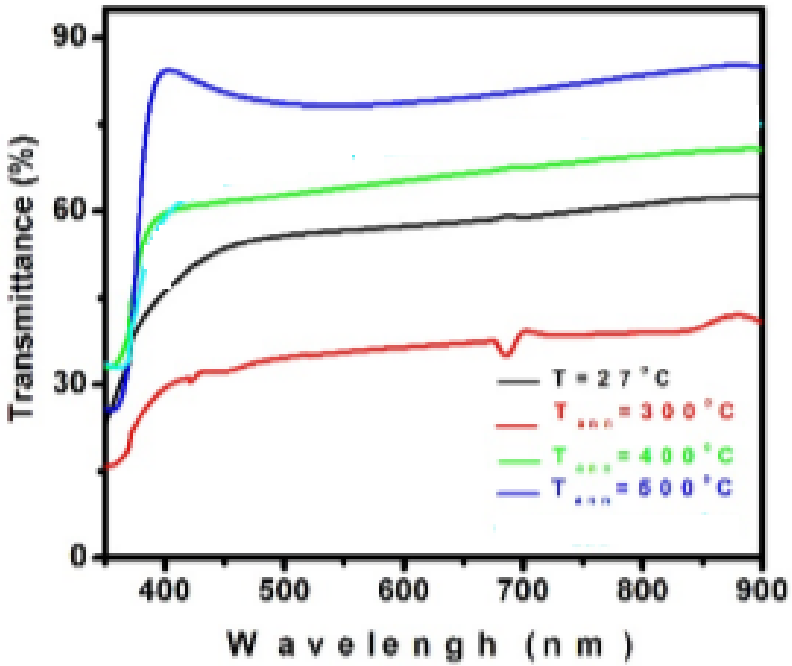

Fig.4 Optical transmittance spectra of as-deposited and post annealed ZnS thin films prepared under vacuum condition

The films with higher surface roughness can reduce the transparency of the films. However the rms surface roughness of the as-deposited film and the film annealed at 300 ^{0}C are almost comparable. The films with mixed phases also may have lesser transparency. But in this case both as-deposited film and the film annealed at 300 ^{0}C have a homogeneous crystalline phase. i.e.; hexagonal wurtzite phase. The films with lesser thickness show higher transmittance. The as-deposited film has a thickness of ~ 68 nm whereas the film annealed at 300 ^{0}C has a thickness of 45 nm. In spite of all these factors the film annealed at 300 ^{0}C shows lesser transmittance compared to that of the as–deposited film and we cannot offer an exact explanation for the unusual behavior of the film. However in the film annealed at 300 ^{0}C consist of compactly arranged grains of smaller size (Fig.2). As the size of the grains decreases, the number density of grain boundaries increases and this may lead to increased scattering loss there by decreasing transmittance.

ZnS is known to be II-VI semiconductor with a direct band gap. The optical band gap E_g can be estimated from the Tauc plot $(\alpha h\nu) = A\,(h\nu - Eg)^n$ (4)

where E_g is the band gap corresponding to a particular transition occurring in the film, A is a constant, ν is the transition frequency and the exponent n characterizes the nature of band transition. For crystalline semiconductors, n can take values1/2, 3/2, 2 or 3 depending on whether the transitions are direct allowed, direct forbidden, indirect allowed and indirect forbidden transitions respectively . The exact values of band gap were determined by extrapolating the straight line portion of the $(\alpha h\nu)^{1/n}$ versus hν graphs to the hν axis, where α is the optical absorption coefficient, hν is the incident photon energy and n depends on the kind of optical transition.

It is found that the band gap values were increased due to the decreased particle size. The energy band gap of a semiconductor depends on the crystal size and its value will increases with a decrease in crystal size due to the quantum confinement effect. It is well known that the energy band gap of a semiconductor is affected by the residual strain, defects, charged impurities, disorder at the grain boundaries [21] and also particle confinement [22].

There is possibility of structural defects in the films due to their preparation at room temperature; this could give rise to the allowed states near the conduction band in the forbidden region. The enhancement in band gap in the case of annealed films is due to the quantum size effect. It is expected that the annealing of the layers might increase the band gap as the annealing process could decrease the disorder present in the layers. In these nanocrystalline layers the grain boundaries might be the dominant source for the presence of structural disorder [23].

The photoluminescence spectra of the ZnS thin films are recorded at room temperature at two excitation wavelengths 250 nm and 325 nm and the emission spectra of as deposited and films annealed at temperatures 300, 400, 500 and 600 ^{0}C is shown in Fig.5. Maximum PL emission occurs for the as-deposited ZnS thin films. With 250 nm excitation, the PL spectra show a broad intense peak at 395 nm and two weak peaks at 452 nm and 469 nm for all the films. As the annealing temperature increases, the intensity of PL peak decreases except for 600 ^{0}C annealing. The spectra showed emission peaks at 534 nm, 578 nm, 443 nm, and 467 nm respectively, when the excitation wavelength is 325 nm. No considerable shift in emission wavelength could be observed with annealing. The luminescence peak around 395 nm is associated with the zinc vacancies and the emission at 443 nm is ascribed to S vacancies. The 534 nm emission has been attributed to elemental sulfur species on the surface of the sample. In semiconductor materials the luminescence can be observed due to excitonic and trapped emissions. Excitonic emission is sharp and located near the absorption edge and trap-state emission is broad and located at longer wavelength regions. The as deposited and the annealed films show different luminescent intensities, which may be related to the different surface roughness of the films and it is inferred from the AFM analysis. The low intensity luminescence peaks observed in the films might be attributed to inter impurity transitions and larger stoichiometric deviations in the films. The luminescence peak was observed at an energy lower than the optical band gap except for all the films, indicating the presence of impurity states in the mid band gap region. This type of luminescence is due to emissions associated with the vacancy states.

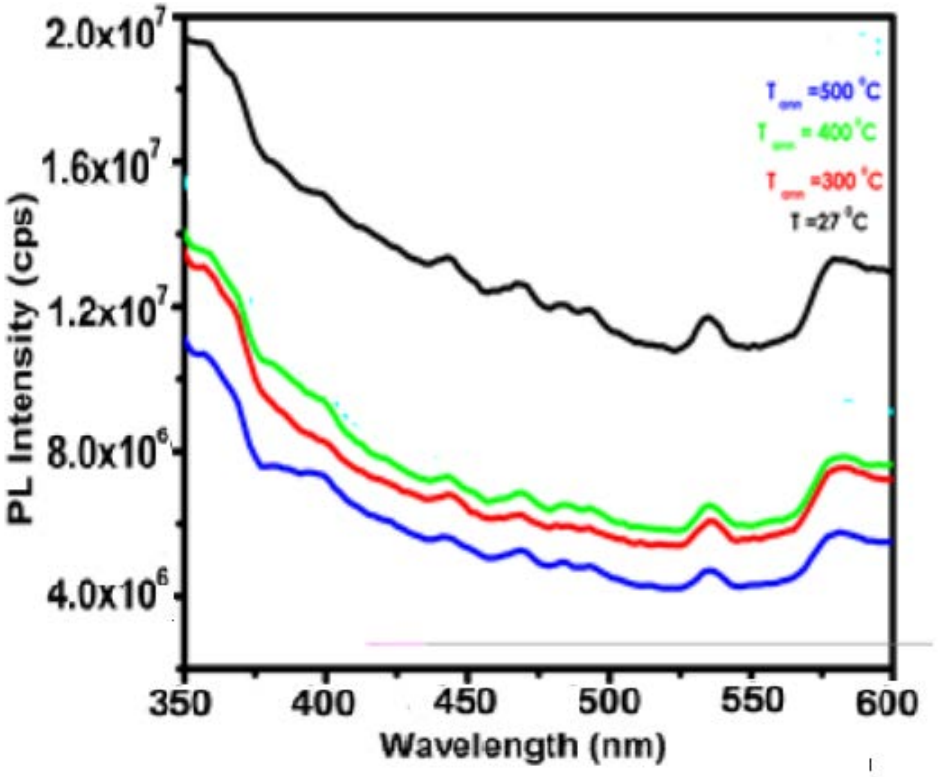

Fig.6 Photoluminescence spectra of as-deposited and post annealed ZnS thin films (A)Excitation 250 nm (B) Excitation 325 nm

4. CONCLUSIONS

Nanocrystalline ZnS thin films have been synthesized by pulsed laser deposition technique. Microstructural and optical studies of as deposited and films annealed at different temperatures are done. From the XRD patterns it is observed that the films prepared under vacuum condition in the as-deposited and annealed form show polycrystalline nature showing hexagonal wurtzite phase. It is found that annealing temperature has profound effect on the structural properties of ZnS films. The average grain size calculated from the XRD pattern of all the films suggests that the grains are in the nano-dimension. The XRD pattern of the film annealed at 600 ^{0}C show a less intense XRD peak of hexagonal ZnO. The AFM images is in support of this XRD observation. A systematic increase of rms surface roughness with increase in annealing temperature is observed. All the films show good transmittance in the visible and near infrared region. It is observed that the band gap energy of the films increases with decrease in particle size and is due to the quantum size effect.The luminescence peak around 395 nm is

associated with the Zinc vacancies . The emission peak at 578 nm is rarely observed by others. The low intensity luminescence peaks observed in the films might be attributed to inter impurity transitions and larger stoichiometric deviations in the films.

References

1. E. Monroy, F. Omnes and F. Calle; Semicond.Sci.Technol., **18** (2003) R33
2. R.N. Bhargava, D. Gallagher, X. Hong and D. Nurmikko; Phys.Rev.Lett., **72** (1994) 416
3. W. Park, J.S. King, C.W. Neff, C. Liddell, and C. Summers; Phys.Status.Solidi., b **229** (2002) 949
4. B. Elidrissi, M. Addou, M. Regragui, A. Bougrine, A. Kachoune and J.C. Bernecde; Mater.Chem.Phys., **68** (2001) 175
5. J. A. Ruffner, M. D. Hilmel, V. Mizrahi, G. I. Stegeman and U. J.Gibson; Appl. Opt., **28** (1989) 5209
6. A. M. Ledger; Appl. Opt., **18 (**1979) 2979
7. W.H Bloss, F.Pfisterer, H.W Schock;"Advances in solar energy, an annual review of research and development"., **4** 275
8. Y. F. Nicolau, M. Dupuy, M Brunel ; J. Electrochem. Soc.,**137** (1990) 2915
9. E. Marquerdt, B.Optiz, M. Scholl, M. Henker ; J.Appl.Phys.,**75** (1994) 8022
10. Jasim M. Abbas, Charita Mehta, G.S.S. Saini, S.K. Tripathi ; Digest Journal of Nanomaterials and Biostructures., **2** (2007) 271-276
11. William Glass Glass, Ajay Kale, Nigel Shepherd, Mark Davidson,David DeVito and Paul H. Holloway ;J.Vac.Sci.Technol.A., **25** (2007) 492-499
12. S.K.Mandal, S.Chaudhuri and A.K.Pal ;Thin Solid Films.,**350** (1999) 209
13. J.Fang,P.H.Holloway,J.E.Yu and K.S.Jones ;Appl.Surf.Sci.,**70/71** (1993) 701
14. K.Uchino,K.Ueyama, M.Yamamoto, H.Kariya, H.Miyata, H.Misasa, M.Kitagawa and H.Kobayashi ;J.Appl.Phys.,**87** (2000) 4249
15. C.T.Hsu ;Thin Solid Films.,**335** (1998) 284],sol-gel[W.Tang and D.C.Cameron ; Thin Solid Films.,**280** (1996) 221

16. B.Elidrissi, M.Addou, M.Regragui, A.Bougrine, A.Kachouane and J.C.Bernede ; Mater.Chem.Phys.**68** (2001) 179

17. K.M.Yeung,W.S.Tsang,C.L.Mark and H.Wong ;J.Appl.Phys.,**92** (2002)3636-3640

18. Zhi-Jun Xin,Richard J Peaty,Harvey N Rutt and Robert W Eason ;Semicond.Sci.Technol., **14** (1999) 695-698

19. H.C. Le, R.W. Dreyfus, W. Marine, M. Sentis, I.A. Movtchan ; Appl.Surf.Sci., (1996) 164

20. X T Zhang, Y C Liu, L G Zhang, J Y Zhang, Y M Lu, D Z Shen, W Xu, G Z Zhong, X W Fan, and X G Kong; J.Appl.Phys., **92** (2002) 3293 3298

21. J.Tauc; Amorphous and Liquid Semiconductors.,Plenum, London, (1974) 159

22. J.R.Rani, V.P.Mahadevan Pillai, R.S.Ajimsha, M.K.Jayaraj, R.S.Jayasree; J.Appl.Phys., **100** (2006) 014302

23. D. Dow and D. Redfield; Phys. Rev., B **5** (1972) 594